

Energy of the quasi-free electron in supercritical argon near the critical point

C.M. Evans^{1,*} and G.L. Findley^{2,†}

¹*Department of Chemistry and Biochemistry, Queens College – CUNY,
Flushing, NY 11367, United States and Department of Chemistry,
Graduate Center – CUNY, New York, NY 10016, United States*

²*Department of Chemistry, University of Louisiana at Monroe, Monroe, LA 71209, United States*
(Dated: June 17, 2005)

Field ionization of high- n CH₃I Rydberg states doped into argon is presented as a function of argon number density along the critical isotherm. These data exhibit a decrease in the argon induced shift of the dopant ionization energy near the critical point. We show that this decrease is due to the interaction between argon and the quasi-free electron arising from field ionization of the dopant. The energy of the quasi-free electron in argon near the critical point is calculated in a local Wigner-Seitz model containing no adjustable parameters to within $\pm 0.2\%$ of experiment.

PACS numbers: 33.15.Ry,34.30.+h,31.70.-f,31.70.Dk

Supercritical fluids have been shown to improve rates and modify product ratios of chemical reactions [1], to vary chemical shifts in NMR [1, 2], and to alter lifetimes and energies of molecular vibrational and electronic states [2]. However, the detailed nature of the molecule (i.e., dopant)/fluid (i.e., perturber) interactions that lead to these effects is not well understood. Due to their “large orbital” nature, Rydberg states are extremely sensitive to their surroundings and, therefore, make excellent probes for studies of dopant/perturber interactions.

In this Letter, we report the field ionization of CH₃I high- n Rydberg states in supercritical argon along the critical isotherm near the critical density. These data show a *decrease* in the perturber induced shift of the dopant ionization energy near the critical density, which contrasts with the *increase* in the density dependent solvatochromic shift of vibrational and UV-visible absorption bands reported by numerous groups [2] in various perturbers. This striking difference stems from the nature of the dopant/perturber interactions in the two cases: the density dependent energy shift of vibrational and UV-vis absorption bands is primarily sensitive to the local density and polarizability of the perturbing medium, whereas the density dependent shift of the dopant ionization energy $\Delta_D(\rho_P)$ in dense media can be written as a sum of contributions

$$\Delta_D(\rho_P) = V_0(\rho_P) + P_+(\rho_P). \quad (1)$$

In this expression, $P_+(\rho_P)$ is the shift due to the average polarization of the perturber by the ionic core, $V_0(\rho_P)$ is the quasi-free electron energy in the perturbing medium, and ρ_P is the perturber number density. While $P_+(\rho_P)$ shifts in a manner similar to that observed for vibrational and UV-visible bands [2], $V_0(\rho_P)$ does not. Thus, the

difference between the perturber induced shift of ionization energy (and of high- n Rydberg state energies) and that of vibrational and UV-visible state energies near the critical point of the perturber is due to the interaction of the quasi-free electron with the perturbing medium. We will show that $V_0(\rho_P)$ and $\Delta_D(\rho_P)$ along the critical isotherm can be accurately modeled to within $\pm 0.2\%$ of experiment using a statistical mechanical calculation for $P_+(\rho_P)$ [3, 4] and a recently developed local Wigner-Seitz model [4] for $V_0(\rho_P)$.

CH₃I/Ar was chosen for this study of supercritical effects on $V_0(\rho_P)$ because the field ionization of CH₃I in dense argon along noncritical isotherms has been well characterized [3–5]. CH₃I (Aldrich, 99.45%) and argon (Matheson Gas Products, 99.9999%) were used without further purification. The absence of trace impurities in the spectral range of interest was verified by the measurement of low density absorption spectra of CH₃I, and of both low density and high density absorption spectra of argon. Field ionization measurements were performed using monochromatized synchrotron radiation [6] having a resolution of 0.9 Å (8 meV in the spectral region of interest). The copper experimental cell, which has a pathlength of 1 cm, is equipped with entrance and exit MgF₂ windows and a pair of parallel plate electrodes (stainless steel, 3 mm spacing) oriented perpendicular to the windows [6]. This experimental cell, which is capable of withstanding pressures of up to 100 bar, is attached to an open flow cryostat and resistive heater that allowed the temperature to be controlled to within $\pm 0.2^\circ\text{C}$. In order to prevent liquid formation in the cell during temperature stabilization, the set point for the critical isotherm was chosen to be -121.7°C , near the argon critical temperature of -122.3°C . The intensity of the synchrotron radiation exiting the monochromator was monitored by measuring the current across a Ni mesh intercepting the beam prior to the experimental cell. All photoionization measurements were normalized to this current. Field ionization spectra were also energy cor-

*cevans@forbin.qc.edu

†findley@ulm.edu

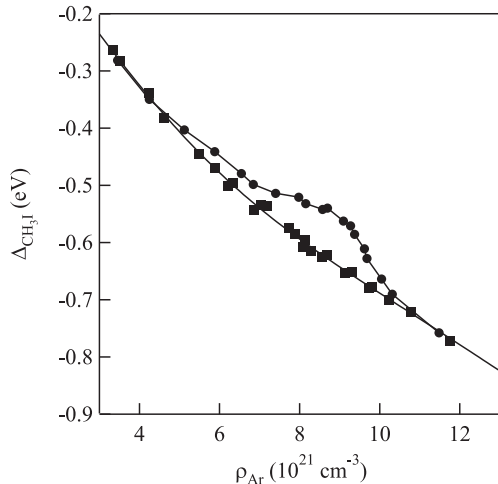


FIG. 1: The experimental argon-induced shift of the CH₃I ionization energy $\Delta_{\text{CH}_3\text{I}}(\rho_{\text{Ar}})$ plotted as a function of argon number density at (■) various noncritical temperatures [4] and (●) along the critical isotherm. The solid lines are provided as a visual aid.

rected for the effects of both the low field F_L and high field F_H (used to generate the field ionization measurement [3]) by $I_0(\rho_P) = I_F(\rho_P) + c_D(F_L^{1/2} + F_H^{1/2})$, where $I_0(\rho_P)$ is the zero-field dopant ionization energy, $I_F(\rho_P)$ is the dopant ionization energy perturbed by the electric field, and $c_D = 4.3 \times 10^{-4} \text{ eV cm}^{1/2} \text{ V}^{-1/2}$ for CH₃I [4]. Both the gas handling system and the procedures employed to ensure homogeneous mixing of the dopant and perturber have been described previously [3, 4, 6]. Prior to the introduction of CH₃I, the experimental cell and gas handling system were baked to a base pressure of 10^{-9} Torr, and in order to ensure no perturber contamination by the dopant (which was present at a concentration of < 10 ppm), the gas handling system was allowed to return to the low 10^{-7} Torr range before the addition of argon.

Fig. 1 presents the argon induced shift of the CH₃I ionization energy $\Delta_{\text{CH}_3\text{I}}(\rho_{\text{Ar}})$ near the critical isotherm of argon, in comparison to that on noncritical isotherms [4]. These data show a clear decrease in the density dependent shift of $\Delta_{\text{CH}_3\text{I}}(\rho_{\text{Ar}})$ near the argon critical density ($\rho_{\text{Ar}} = 8.0 \times 10^{21} \text{ cm}^{-3}$). In order to determine $V_0(\rho_{\text{Ar}})$ experimentally from Eq. (1), the average ion-perturber polarization energy $P_+(\rho_{\text{Ar}})$ must be evaluated. We chose to calculate $P_+(\rho_{\text{Ar}})$ using [3, 4]

$$P_+(\rho_P) = -4\pi\rho_P \int_0^\infty g_{\text{PD}}(r) w_+(r) r^2 dr, \quad (2)$$

where $g_{\text{PD}}(r)$ is the perturber/dopant radial distribution function, and $w_+(r)$ is given by [3, 4]

$$w_+(r) = -\frac{1}{2} \alpha_P e^2 \sum_i^N r_i^{-4} f_+(r_i). \quad (3)$$

In the above equation, α_P is the polarizability of the per-

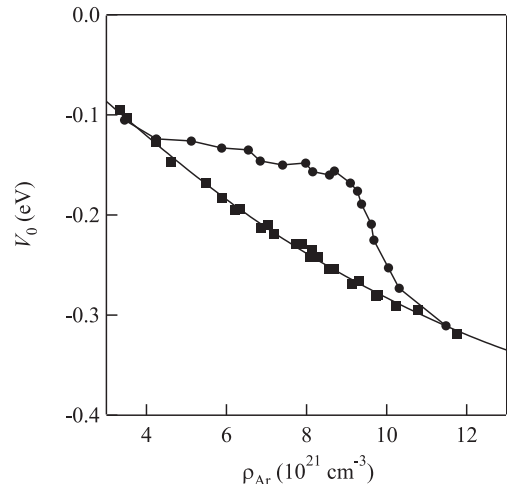


FIG. 2: $V_0(\rho_{\text{Ar}})$, determined from Eq. (1) by subtracting $P_+(\rho_{\text{Ar}})$ from the experimentally determined argon-induced shift of the CH₃I ionization energy $\Delta_{\text{CH}_3\text{I}}(\rho_{\text{Ar}})$ in Fig. 1, plotted as a function of argon number density at (■) various noncritical temperatures [4] and (●) along the critical isotherm. The solid lines are provided as a visual aid.

turber, e is the electron charge, and $f_+(r)$ is a screening function that incorporates the repulsive interactions between the induced dipoles in the perturber medium [3, 4, 7]. Since $f_+(r)$ involves induced dipole interactions in the perturbing medium, $f_+(r)$ incorporates the perturber/perturber radial distribution function g_{PP} . The radial distribution function $g_{\text{PD}}(r)$, which reflects the distribution of perturber (i.e., argon) atoms around the ground state dopant molecule (i.e., CH₃I), was computed from the coupled Percus-Yevick integral equations [4, 8] for a modified Stockmeyer potential written in Lennard-Jones 6-12 form [4, 9] with $\sigma_{\text{PD}} = 4.074 \text{ \AA}$ and $\varepsilon_{\text{PD}}/k_B = 162.2 \text{ K}$ (where k_B is Boltzmann's constant) [4]. The perturber/perturber radial distribution function g_{PP} was determined using the same Percus-Yevick integral equations [4, 8], but for a standard Lennard-Jones 6-12 potential with $\sigma_{\text{PP}} = 3.409 \text{ \AA}$ and $\varepsilon_{\text{PP}}/k_B = 119.5 \text{ K}$ [4]. The screening function $f_+(r)$ was evaluated numerically, as described in [3], using our results for the radial distribution functions and $\alpha_{\text{Ar}} = 1.64 \text{ \AA}^3$ [10]. Subtracting $P_+(\rho_{\text{Ar}})$ from $\Delta_{\text{CH}_3\text{I}}(\rho_{\text{Ar}})$ leads to the experimental values of $V_0(\rho_{\text{Ar}})$ for the critical isotherm data, which are presented in Fig. 2 and compared to the noncritical isotherm data [4]. It is clear from Fig. 2 that the energy of the quasi-free electron (i.e., the energy of the bottom of the conduction band in argon) varies considerably near the critical point. This variation in the quasi-free electron energy may well have a bearing on the changes in reactivity [1, 2] and product distribution [1, 2] observed in chemical reactions conducted in certain supercritical fluids.

The behavior of $V_0(\rho_{\text{Ar}})$ along the critical isotherm around the critical density of the perturber is more com-

plex than that along noncritical isotherms. We have recently presented [4] a new local Wigner-Seitz treatment that accurately models $V_0(\rho_{Ar})$ for CH_3I/Ar to within $\pm 0.1\%$ of experiment along the noncritical isotherms. As in previous treatments of the quasi-free electron, this model begins with the one-electron Schrödinger equation

$$\left[-\frac{\hbar^2}{2m} \nabla^2 + V(r) - E \right] \psi = 0, \quad (4)$$

where $V(r)$ is the one-electron potential exerted by the neat fluid. As in the original Springett, Jortner and Cohen (SJC) [11] model, we also assume that this potential is spherically symmetric about the perturber, and that (neglecting fluctuations) it has an average translational symmetry. However, our model does not assume that the average distance between atoms in a dense gas can be determined by dividing the volume into spheres defined by the Wigner-Seitz radius [4, 11] obtained from the bulk number density. In dense gases, one does not have a uniform distribution of perturbers because of perturber/perturber interactions. Thus, the translational symmetry boundary condition must reflect this nonuniformity. One way to meet this requirement is to obtain the local number density from the radial distribution function, since [12, 13]

$$\rho_P(r) = g_{PP}(r) \rho_P, \quad (5)$$

where $\rho_P(r)$ is the local perturber number density, and ρ_P is the bulk perturber number density. In this case, then, the translational symmetry is defined by a local Wigner-Seitz radius [4]

$$r_\ell = \sqrt[3]{\frac{3}{4\pi g_{\max} \rho_P}} \quad (6)$$

where g_{\max} is the maximum of the radial distribution function. The local Wigner-Seitz radius, therefore, represents one-half the average spacing between rare gas atoms in the first solvent shell. As in the SJC model [11], we assume that $V(r)$ is divided into two parts: an attractive electron/perturber polarization energy $P_-(\rho_P)$, which is similar to $U_p(\rho_P)$ in the SJC model [11], and a repulsive atomic pseudopotential $V_a(r)$.

We calculate the attractive electron/perturber polarization energy $P_-(\rho_P)$ in a manner similar to that given for the ion polarization potential $P_+(\rho_P)$ in Eqs. (2) and (3), but with an interaction potential originally proposed by Lekner [7],

$$w_-(r) = -\frac{1}{2} \alpha_P e^2 \sum_i^N r_i^{-4} f_-(r_i), \quad (7)$$

where $f_-(r_i)$ is a screening function given by

$$f_-(r) = 1 - \pi \alpha_P \rho_P \int_0^\infty \frac{1}{s^2} g_{PP}(s) ds - \int_{|r-s|}^{r+s} \frac{1}{t^2} f_-(t) \theta(r, s, t) dt, \quad (8)$$

with $\theta(r, s, t)$ defined by

$$\theta(r, s, t) = \frac{3}{2s^2} (s^2 + t^2 - r^2) (s^2 - t^2 + r^2) + (r^2 + t^2 - s^2). \quad (9)$$

The average electron/perturber polarization energy can then be obtained from [4]

$$P_-(\rho_P) = -4\pi \rho_P \int_0^\infty g_{PP}(r) w_-(r) r^2 dr. \quad (10)$$

The potential $V(r)$ in Eq. (4) therefore becomes $V(r) = V_a(r) + P_-(\rho_P)$, where $P_-(\rho_P)$ is a constant for a fixed perturber number density. As in the SJC treatment [11], we define $V_a(r)$ as a hard core potential (i.e., $V_a(r) = 0$ for $r > r_h$ and $V_a(r) = \infty$ for $r < r_h$, where r_h is the hard core radius), but we set r_h equal to the absolute value of the scattering length A of the perturber. Finally, a phase shift is introduced to reflect the fact that outside the first solvent shell the quasi-free electron wavefunction can also scatter off the rare gas atoms contained within the solvent shell. For s -wave scattering, and in the limit of small k_0 , this phase shift is given by $\eta\pi$, where η is the phase shift amplitude [14]. Incorporating this phase shift into the solution to Eq. (4) under the boundary conditions

$$\psi_0(|A|) = 0, \quad \left. \left(\frac{\partial \psi_0}{\partial r} \right) \right|_{r=r_\ell} = 0, \quad (11)$$

yields the wavevector equation for the quasi-free electron:

$$\tan [k_0(r_\ell - |A|) + \eta\pi] = k_0 r_\ell. \quad (12)$$

In this model, η is a perturber dependent parameter that is evaluated from the field ionization and/or photoconduction data for $V_0(\rho_P)$ from the noncritical isotherm experiments [4]. Once the thermal kinetic energy of the quasi-free electron is included, $V_0(\rho_P)$ becomes

$$V_0(\rho_P) = \frac{(\hbar k_0)^2}{2m} + P_-(\rho_P) + \frac{3}{2} k_B T, \quad (13)$$

where k_0 is evaluated from Eq. (12).

Fig. 3a presents $V_0(\rho_{Ar})$ obtained from Eq. (13), with $\eta = 0.40$ [4] and $A = -0.82 \text{ \AA}$ [6], for the critical isotherm (open markers) in comparison to the experimentally determined values (solid markers) [cf. Fig. 2]. (A nonlinear least squares fit to the noncritical isotherm data [4] (solid line) is included in Fig. 3a as an aid to the eye.) Clearly, the calculated $V_0(\rho_{Ar})$ closely matches experiment, with a scatter of $\pm 0.2\%$ of experiment that easily falls within the overall experimental error of $\pm 0.02 \text{ eV}$. Finally, Fig. 3b presents the calculated $\Delta_{CH_3I}(\rho_{Ar})$ along the critical isotherm (open markers), using $P_+(\rho_{Ar})$ obtained from Eq. (2) and $V_0(\rho_{Ar})$ obtained from Eq. (13), in comparison to the experimentally determined values

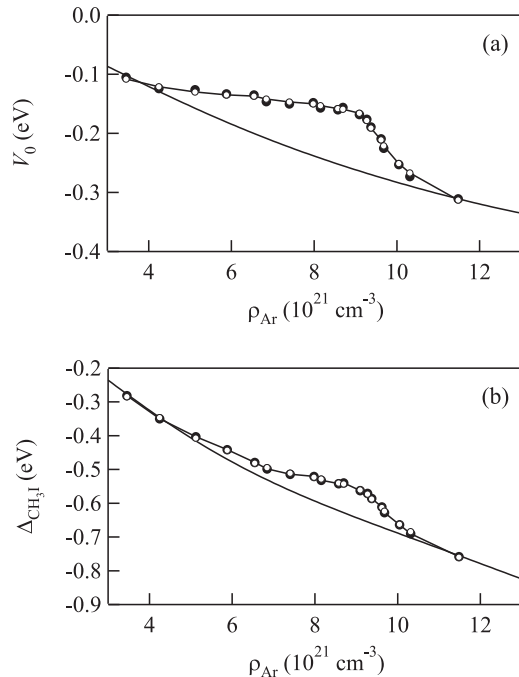


FIG. 3: Comparison of experiment (●) and calculation (○) for (a) the energy of the quasi-free electron in argon $V_0(\rho_{Ar})$ and for (b) the argon induced shift of the CH_3I ionization energy $\Delta_{\text{CH}_3\text{I}}(\rho_{Ar})$, plotted as a function of argon number density ρ_{Ar} on the argon critical isotherm. The solid lines are nonlinear least squares fits (using a seventh order polynomial function) to the noncritical isotherm data [4] and are provided as a visual aid.

(solid markers) [cf. Fig. 1]. (The nonlinear least squares fit to the noncritical isotherm data [4] (solid line) is reproduced in Fig. 3b as an aid to the eye.) Again, the calculated $\Delta_{\text{CH}_3\text{I}}(\rho_{Ar})$ closely matches experiment, with a scatter of $\pm 0.2\%$ of experiment that easily falls within the overall experimental error of ± 0.02 eV. It is important to note that there are no adjustable parameters in this model for the critical isotherm data, since η was determined from the noncritical isotherm data [4].

In summary, we have shown that the behavior of the perturber induced shift of the dopant ionization energy (and, therefore, the high- n Rydberg state energies) differs significantly from the previously reported [2] energy shifts in vibrational and UV-visible absorption bands near the critical point of a perturber, and we have explained this difference as arising from the interaction of the quasi-free electron with the perturbing medium. Moreover, we have also shown that a recently developed local Wigner-Seitz model [4] predicts $V_0(\rho_{Ar})$ and $\Delta_{\text{CH}_3\text{I}}(\rho_{Ar})$ to within $\pm 0.2\%$ of experiment near the criti-

cal density along the critical isotherm with no adjustable parameters. While we have restricted ourselves here to a single dopant/perturber system, the differences seen in $\text{CH}_3\text{I}/\text{Ar}$ near the critical point have also been observed in $\text{C}_2\text{H}_5\text{I}/\text{Ar}$ [15], and in CH_3I and $\text{C}_2\text{H}_5\text{I}$ in Kr [16].

We are grateful to Dr. Ruben Reininger (University of Wisconsin Synchrotron Radiation Center) for many helpful discussions. We thank Luxi Li (Queens College) for her assistance in the calculations contained in Fig. 3. The experimental measurements reported here were performed at the University of Wisconsin Synchrotron Radiation Center (NSF DMR-0084402). This work was supported by grants from the Louisiana Board of Regents Support Fund (LEQSF (1997-00)-RD-A-14), from the Petroleum Research Foundation (41378-G6), and from the Professional Staff Congress City University of New York (60073 - 34 35).

-
- [1] O. Kajimoto, Chem. Rev. **99**, 355 (1999), and references therein.
 - [2] S. C. Tucker, Chem. Rev. **99**, 391 (1999), and references therein.
 - [3] A. K. Al-Omari, Ph.D. dissertation, University of Wisconsin Madison (1996), see also A. K. Al-Omari, K. N. Altmann and R. Reininger, J. Chem. Phys. **105**, 1305 (1996).
 - [4] C. M. Evans and G. L. Findley, Phys. Rev. A (2005), accepted.
 - [5] I. T. Steinberger, in *Classical Rare Gas Liquids*, edited by W. F. Schmidt and E. Illenberger (Am. Sci. Publ., in press).
 - [6] C. M. Evans, Ph.D. dissertation, Louisiana State University (2001), see also C. M. Evans, J. D. Scott and G. L. Findley, Rec. Res. Dev. Chem. Phys. **3**, 351 (2002).
 - [7] J. Lekner, Phys. Rev. **158**, 158 (1967).
 - [8] E. W. Grundke, D. Henderson, and R. D. Murphy, Can. J. Phys. **51**, 1216 (1973).
 - [9] J. O. Hirschfelder, C. F. Curtiss, and R. B. Bird, *Molecular Theory of Gases and Liquids* (Wiley, New York, 1954).
 - [10] D. R. Lide, ed., *CRC Handbook of Chemistry and Physics, 84th edition* (CRC Press, Boca Raton, 2004).
 - [11] B. E. Springett, J. Jortner, and M. H. Cohen, J. Chem. Phys. **48**, 2720 (1968).
 - [12] P. Attard, J. Chem. Phys. **91**, 3072 (1989).
 - [13] P. Attard, J. Chem. Phys. **91**, 3083 (1989).
 - [14] F. Calogero, *Variable Phase Approach to Potential Scattering* (Academic Press, New York, 1967).
 - [15] C. M. Evans and G. L. Findley, J. Phys. B (2005), submitted.
 - [16] C. M. Evans and G. L. Findley, J. Phys. Chem. A (2005), to be submitted.